* First Place Winner in 1995 Roon Awards Competition *

Latex Blends: An Approach to Zero VOC Coatings

Mitchell A. Winnik and Jianrong Feng—University of Toronto*

An attractive strategy for zero VOC coatings involves blends of hard and soft latex particles. A dispersion of a latex with a low minimum film-forming temperature will form a transparent film upon evaporation, even when blended with a substantial amount of high T_g latex. The low T_g latex deforms to fill space as the dispersion dries, and the high T_g component imparts good block resistance and mechanical properties to the final film. Transparency requires that the hard latex be sufficiently small and well dispersed in the final film. In addition, the two components must have similar refractive indices. Two of our most surprising observations are that dispersions of soft latex particles dry more slowly than those of high T_g latex, and that mixtures of the two particles dry even more slowly. Consideration of these results leads to a new model for the drying mechanism of latex dispersions that takes into account the propagating drying front. Dynamic mechanical analysis indicates that the hard particles in blends improve significantly the mechanical properties for the films.

INTRODUCTION

Concern for the environment is leading to changes in coatings technology. In the U.S. and around the world, agencies are in the process of implementing increasing limitations on the emission of volatile organic compounds (VOCs). These emissions are believed to be the primary cause of photochemical smog and ozone pollution. A significant portion of the VOCs currently released into the atmosphere derive from industrial and architectural paints and coatings. The coatings industry has responded to this challenge by trying to replace solvent-based coatings either with water-borne or high-solids systems.[1,2]

Even within water-based systems, volatile organics are used to promote coalescence. These film-forming aids lower the modulus of the latex polymer to promote particle deformation during drying, and they act as plasticizers to promote polymer diffusion in the newly formed film.[1,3] In this way they enhance the development of good film properties. If they remained within the resin, the film would be soft and have poor mechanical properties and poor block resistance. In this technology, good film properties are achieved when the solvent evaporates from the film into the atmosphere.

A number of strategies are currently being tested which will lead to film formation from aqueous latex dispersions without the need for volatile additives. One of the most attractive of these involves blends of hard and soft latex.[4,5] A dispersion of a latex with a glass transition temperature (T_g) below room temperature (a low T_g latex) will form a continuous film upon evaporation at room temperature, even when blended with a substantial amount of high T_g latex. The low T_g polymer deforms to fill space as the dispersion dries, and the high T_g component imparts good block resistance to the final film. Under some circumstances one can obtain transparent films. As we shall see in the following, this result requires that the hard latex be sufficiently small and well dispersed within the matrix of the soft polymer and that the refractive indices of the two latex polymers be similar.

Although the topic of latex blends is actively being investigated in the industry, there have been few publications which examine the formation and properties of latex blend films. These blends provide a number of surprises, which are important from both a scientific and technological point of view. One of the most interesting concerns is how these blended dispersions dry.

The body of this paper is divided into five parts which follow a short Experimental Section. The first presents the idea of a transparency phase diagram, and examines the surface and bulk morphology of blend films. As the fraction of low T_g latex in the dispersion is increased, there is a sharp transition from turbid to transparent films. The subsequent

Presented at the 73rd Annual Meeting of the Federation of Societies for Coatings Technology, on October 9, 1995, in St. Louis, MO.

*Department of Chemistry and Erindale College, 80 St. George St., Toronto, Ont., M5S 1A1, Canada.

Table 1—PMMA Latex Characteristics

Sample	PMMA Latex				
Diameter (nm)	44	110	167	230	400
Polydispersity	0.005	0.005	0.005	0.005	0.005
Mw ($x10^{-5}$)	4.6	2.1	—	—	—
Mw/Mn	2.0	2.3	—	—	—

three sections, which are the main contributions of this paper, examine in detail the drying behavior of single-component and blended dispersions. We emphasize an important feature that latex dispersions dry with a drying front, which separates a dry film part from a wet dispersion region and propagates directionally as the drying proceeds. We report and explore the finding that blends of hard and soft latex dry more slowly than either individual dispersion. This kind of rate difference can only occur if the drying rate is not controlled by the wet region, but by the boundary between the wet and dry regions of the film. From these observations, we develop a new model of the drying process. Finally we look briefly at how the high T_g latex affects the mechanical properties of the blend films.

Some experiments involve blends of poly(methyl methacrylate) [PMMA] as the hard latex with various butyl methacrylate-butyl acrylate copolymer [P(BMA-co-BA)] latex as the low T_g component. Other experiments involve two samples of poly(methyl methacrylate-co-butyl acrylate) [P(MMA-co-BA)] with slightly different compositions, one with T_g = 48°C, the other with T_g = 17°C.

EXPERIMENTAL

The latex samples employed here have been described previously.[4,6] The characteristics of these samples are collected in *Tables* 1-3. To prepare films, latex dispersions were placed on a flat glass substrate or quartz plate and air dried. For some samples, an inverted petri dish was used to cover the drying dispersions to slow the process of film formation. Other samples were dried directly in the open air. The films formed had a thickness of ~ 50 μm.

Measuring Water Loss During Drying

All dispersions were adjusted to an initial solids content of 5 wt%. For each set of samples to be compared, the initial quantities of dispersion (e.g., 0.300 g) were weighed as identically as possible (± 0.3%). The dispersions were spread on individual glass plates to produce wet films with similar surface areas (e.g., 5.0 ± 0.2 cm^2). With practice we could achieve this reproducibility. Films were dried at ambient temperature (22 ± 1°C) and humidity in an area of the laboratory free from drafts. The humidity changed from 45 to 65% relative humidity day to day, but it was fairly constant (with a small deviation < ± 2% relative humidity) during the measurement time of each set of samples. The samples were weighed at regular time intervals using an analytical balance: each half hour at early stages, and each 10-15 min at later stages, of drying. The changes in solids content with time were calculated from the water loss data. In our experiments, the latex drying occurs as a moving front, showing a decrease in surface area of the wet part of the film. A ruler was placed over the film surface after each time interval to measure the dimensions of the wet region.

Table 2—P(BMA-co-BA) Latex Characteristics

Sample	P(BMA-co-BA) Latex			
Diameter (nm)	43	32	38	49
Polydispersity	0.008	0.026	0.017	0.077
T_g[a] (°C)	–33.0	–6.9	4.1	9.9
Mw ($x10^{-5}$)	8.4	6.7	3.5	1.1
Mw/Mn	1.7	1.9	2.4	6.9

(a) Only one T_g was observed by DSC for each copolymer sample.

Film Characterization

Film transparency was monitored with a Hewlitt-Packard model 8452A diode array UV-VIS spectrophotometer (400 to 700 nm). The percent transmittance was recorded at 550 nm. Freeze-fracture transmission electron micrographs (FFTEM) were taken in the laboratory of Professor R.S. Shivers at the University of Western Ontario. Details are given in references 4 and 7. Scanning electron micrographs (SEM) were taken in Toronto using a Hitachi S-570 system under low voltage to prevent the melting of the soft component. Atomic force microscopy (AFM) measurements were carried out in Toronto in the laboratory of Professor J. Vancso using the Nanoscope III in the TappingMode™. Dynamic mechanical analysis (DMA) measurements were performed with a Perkin-Elmer DMA-7 system. Thick films (.025-0.50 mm) were prepared by air drying the dispersions in a Teflon mold and then cutting the films into rectangular pieces (10 mm × 4 mm). Measurements were made in the extension mode to obtain E′, E″, and tan δ.

TRANSPARENCY AND MORPHOLOGY OF BLEND FILMS

Transparency

There are several requirements for transparency in a latex blend film. First, the number of voids in the film that can scatter light must be negligible.[1] This requires complete coalescence of particles for the latex system. In our binary latex system, the hard particles are not able to deform; therefore it is essential that the soft particles deform to fill space, as well as serving as a binder for the hard particles. In addition, the refractive indices of the two polymers must be similar,[8] or, if they differ, the dispersed domain sizes must be small.[9] In the blends described here, the latex particles are rather small. Their refractive indices are unlikely to be very different, based upon the values of the corresponding homopolymers, 1.490 for PMMA, 1.483 for PBMA, and 1.474 for PBA.[10]

Table 3—P(MMA-co-BA) Latex Characteristics

Sample	High T_g Latex	Low T_g Latex
D_n (nm)	111	103
D_w/D_n	1.11	1.10
Mw ($x10^{-5}$)	2.3	2.5
Mw/Mn	2.9	3.1

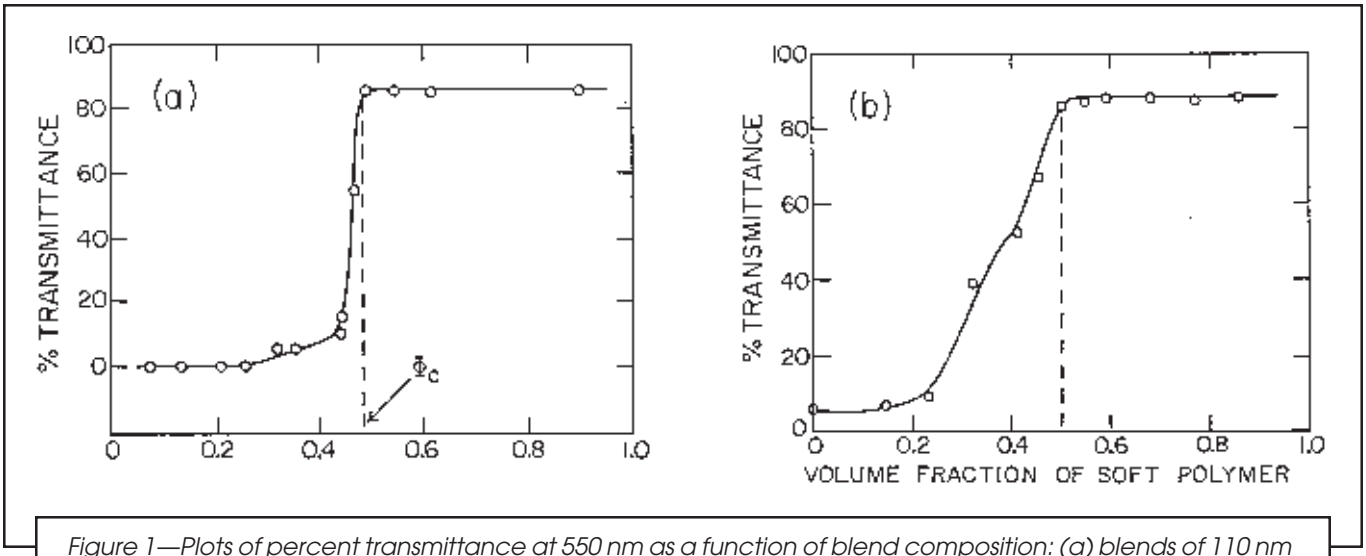

Figure 1—Plots of percent transmittance at 550 nm as a function of blend composition: (a) blends of 110 nm PMMA latex with 38 nm P(BMA-co-BA) latex of T_g = 4.1°C; (b) blends of P(MMA-co-BA) latex of T_g = 48°C with that of T_g = 17°C, both samples of d ~ 110 nm. The dashed line represents our definition of the critical volume fraction of the soft component for film transparency.

We obtained films which are transparent to the eye in blends rich in the soft component. UV-VIS measurements indicate that the transmittance of these samples is on the order of 85 to 95% over the entire visible wavelength range. Turbid samples were obtained from blends rich in hard latex. Here the transmittance is only 5-20%.[4] In all the cases, we found that there is a value of the volume fraction of soft polymer at which we could obtain a clear film, and below which we only could get a turbid film with cracks or, in the extreme, a white powder. We define this as the critical volume fraction of soft polymer, Φ_c, in these composite films.

Figure 1 shows two examples of transparency phase diagrams, i.e., plots of light transmission versus blend composition. The plot in *Figure* 1a describes blends of 110 nm PMMA latex with 38 nm P(BMA-co-BA) latex of T_g = 4.1°C. The transition between turbid and transparent films is extremely sharp. The two components of this blend differ in refractive index by about 0.01, which can be sufficient to scatter light if the hard particles are not well separated in the blend. *Figure* 1b is for blends of P(MMA-co-BA) latex of T_g = 48°C with that of T_g = 17°C, both having a diameter of 110 nm. Here we observe cracks at a soft fraction between 0.3 and 0.5. Since the two components differ in refractive index by only about 0.001, the turbidity seen at lower fractions of soft component likely arises from void scattering.

One might expect that the volume fraction of soft polymer necessary to give transparent films would correspond to that necessary to fill the void volume of close-packed hard spheres. This volume fraction Φ_{soft} would be equal to 0.26 or 0.34 depending upon whether the close packing was face-centered cubic or random. Φ_c values found in our experiments are always above these values and close to 0.5. This implies that the soft polymer forms a continuous phase in transparent films, with the hard particles dispersed in it.

Morphology

Film surface morphologies were examined by scanning electron microscopy (SEM), and in some instances, by atomic force microscopy (AFM). In blends of PMMA and P(BMA-co-BA) particles, SEM images show that transparent films are characterized by a uniform distribution of hard particles in the low T_g matrix. When the hard particles are too large (e.g., 230 or 400 nm), they tend to aggregate during the drying process. It is very difficult to obtain transparent films from these blends. Even when the PMMA latex particles are appropriately small (e.g., 110 nm), if they aggregate during film formation, the resultant films are turbid.

A number of these film samples were examined by FFTEM. This technique provides a rich view of the fracture surface of

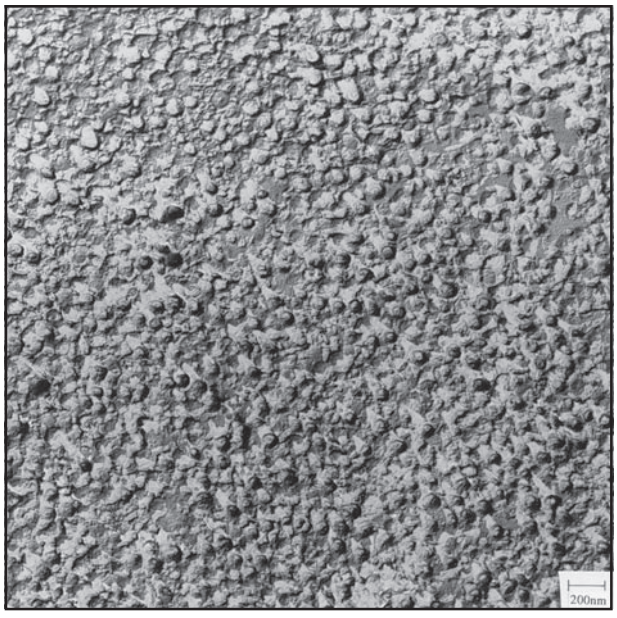

Figure 2—FFTEM image of a latex blend film containing a 1:1 mixture of 110 nm PMMA particles and P(BMA-co-BA) particles of d = 32 nm and T_g of –6.9°C. The film was fractured at –170°C, and shadowed with platinum-carbon.

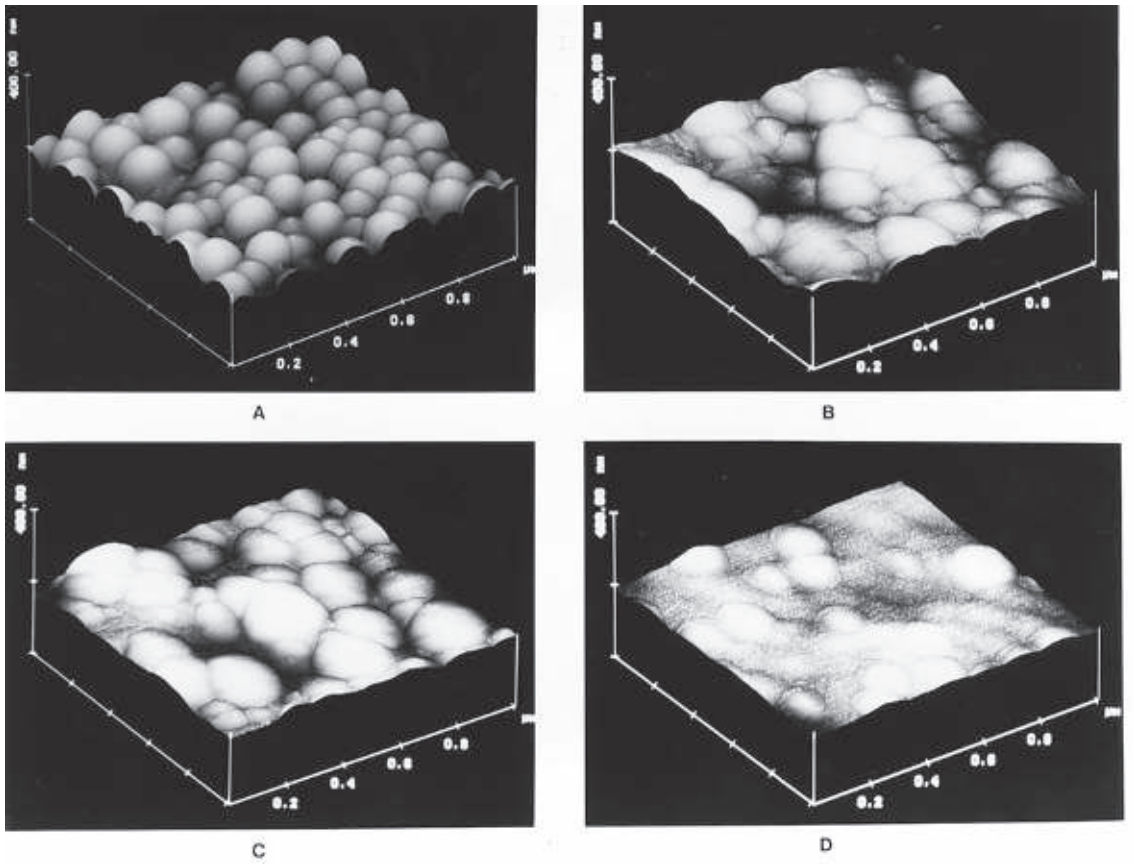

Figure 3—AFM images (three-dimensional, 1 μm × 1 μm × 400 nm) of the surface of blends of high T_g and low T_g P(MMA-co-BA) samples (both d ~ 110 nm) with compositions of Φ_{soft} = (a) 0.2, (b) 0.4, (c) 0.6, and (d) 0.8, respectively.

the film interior with high resolution and with minimal distortion. In *Figure* 2, we present an FFTEM image of a transparent film comprised of a 1:1 mixture of 110 nm PMMA particles and small soft P(BMA-co-BA) latex. One can see that the hard (PMMA) particles preserve their size and spherical shape. The soft particles have deformed and result in a void-free internal structure. The hard particles are uniformly distributed in the soft polymer matrix. These results support the idea that film transparency is dependent on the distribution of hard particles in the soft polymer matrix.

Figure 3 shows AFM images of P(MMA-co-BA) latex blend films of different compositions. In these blends, the hard particles (T_g = 48°C) and soft particles (T_g = 17°C) are of similar size (d = 110 nm). At a soft particle volume fraction of 0.2, the hard particles are still apparent as undeformed spheres, held together by a "glue" of deformed soft particles, as seen in *Figure* 3a. At Φ_{soft} = 0.4 (*Figure* 3b) and 0.6 (*Figure* 3c), further soft particle coalescence can be seen. The most striking feature of these images is the presence of bumps which appear larger than the size of either of the individual hard or soft particles. This may be due to particle clustering. Because the bumps are quite smooth and resemble boulders more than spheres, it is reasonable to suppose that they are formed by coalescence of soft particles over the underlying hard particles. This idea is supported by the observation that as the hard particle volume fraction is decreased, the number of bumps also decreases, as seen in the image for a Φ_{soft} = 0.8 film (*Figure* 3d).

The AFM surface images correlate with the phase diagram shown in *Figure* 1b. In the sample of Φ_{soft} = 0.2 film, void spaces between hard particles are apparent, suggesting the presence of extensive voids within. The phase diagram indicates a transition to void-free films at Φ_{soft} = ca. 0.5. In the AFM images of the Φ_{soft} = 0.4 and Φ_{soft} = 0.6 films, possible voids between particles are much harder to discern. The film surfaces are not very smooth, although the roughness is on the order of a particle diameter. If there is clustering of the higher T_g latex in the sample of Φ_{soft} = 0.6, this would be unlikely to lead to turbidity because of the very small difference of refractive indices between the two polymers. In the sample with Φ_{soft} = 0.8, the soft polymer forms the matrix. There are no voids, and the hard particles are well dispersed.

KINETICS OF DRYING

Most coatings formulations contain latex dispersions at relatively high solids, i.e., > 40 wt%. As a consequence, most previous studies of the drying process began with dispersions at high concentrations. Since we wished to look carefully at the early stages of drying, we chose to dilute all dispersions including blends to 5.0 wt% solids. Some dispersions con-

tained an anionic surfactant (sodium dodecyl sulfate or SDS, 2-6 wt% solids), whereas other dispersions were cleaned carefully to remove all salts and surfactant. In the following paragraphs, we compare the rates of water loss from samples of soft latex, hard latex, and their blends. When examining a given variable, we compare samples prepared to have equal area, mass, and wet film thickness and whose water-loss rates were measured simultaneously. The reproducibility between identical samples examined in this way was excellent, and the data quality can be judged by reference to the figures presented in the following.

Water Evaporation Rate at Low Solids

An example of a water evaporation experiment is shown in *Figure* 4, where we compare mass loss as a function of time from three liquid films: pure water, a soft latex dispersion [P(BMA-co-BA), d = 43 nm, T_g = –33°C], and a hard latex dispersion (PMMA, d = 110 nm). The two dispersions were cleaned to remove surfactant. The first feature that one notices is that water loss over 2/3 of the drying is linear in time. In addition, the water loss curves of pure water and the dispersions overlap in this linear region, indicating an identical drying rate, with a water evaporation rate of $3.5 \pm 0.1 \times 10^{-4}$ g min^{-1} cm^{-2}. This value is not very different from those reported in the literature. Vanderhoff[11] reported in his early paper that latex dispersions dried at a similar rate to thin films of water. Croll[12] found that latex dispersions and various pigment dispersions dried initially at a constant rate which was about 85% of that of pure water. Numerical simulations by Vanderhoff and coworkers using heat and mass transfer equations also gave a similar factor of about 85%.[13] We find a negligible difference in initial drying rates between water and latex dispersions. Note that our latex drying experiments begin at a much lower solids content (5 wt%) than those of Vanderhoff and Croll (ca. 50 wt%).

Drying Front

Published models of latex drying assume that water evaporation occurs uniformly over the entire film surface. In all of our experiments, the films dried as a propagating front. When the dispersions were placed in a small circular dish with a vertical wall, a concave meniscus was formed with a thicker edge near the wall and a thin central region. Here drying takes place first at the center where the liquid is thinnest and moves outward towards the thick edge. Concurrently, drying from the top of the liquid at the wall surface also occurred, progressing downward to the bottom of the dish. The film formed at the bottom of the dish had a much thicker edge (e.g., 200 μm) and a very thin center (e.g., 10 μm).

When the dispersions were spread onto a flat glass surface, a flat liquid drop with a slightly convex surface formed spontaneously. Here the liquid center is relatively thick with a thinner edge. Drying occurs initially at the outermost region, and the dry region grows inward toward the center. We observe this process for both surfactant-containing and surfactant-free dispersions. Films formed on a flat glass surface often have a relatively thicker edge (e.g., 60 μm) surrounding a large flat portion (e.g., 45 μm thick) in the center. With surfactant and salts removed, the ridge at the edge is barely discernible. This kind of drying behavior characterized by a propagating drying front in latex dispersions has been mentioned previously,[14,15] but we wish to emphasize that models of the drying process have not taken the drying front into account.

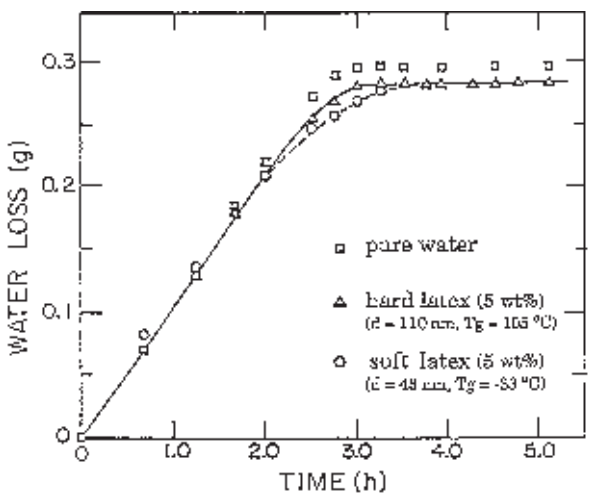

*Figure 4—Water loss as a function of time for water (*squares*), a dispersion of soft latex (*circles*), and of hard latex (*triangles*). In the soft latex: d = 43 nm, T_g = –33°C and in the hard latex: d = 110 nm. The latex samples are surfactant-free, initially at a concentration of 5 wt%.*

Figure 5 illustrates the drying process of our latex dispersions spread on a flat glass surface. A dry region forms at the edge of the film. There is a thin transition region which represents the drying front that separates the dry region from the inner wet dispersion. With time, the drying front moves inward, accompanied by a decrease in surface area of the wet center.

Comparison of Hard and Soft Latex Dispersions

In our experiments, we monitored both water loss and the area of the wet center as a function of time. We are thus able to relate the loss of water and the growth in percent solids to

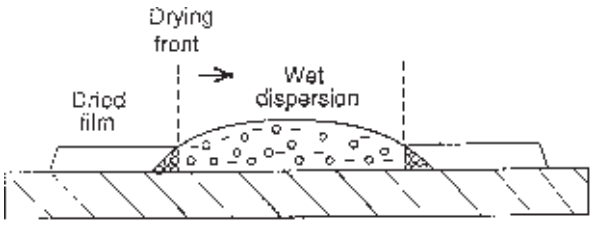

Figure 5—A drawing illustrating film formation on a flat substrate during drying. A transparent film at the edge is separated from an inner wet dispersion by a boundary referred to as the drying front. The drying process is characterized by movement of the drying front towards the center until the wet dispersion fades, and the film is entirely dry.

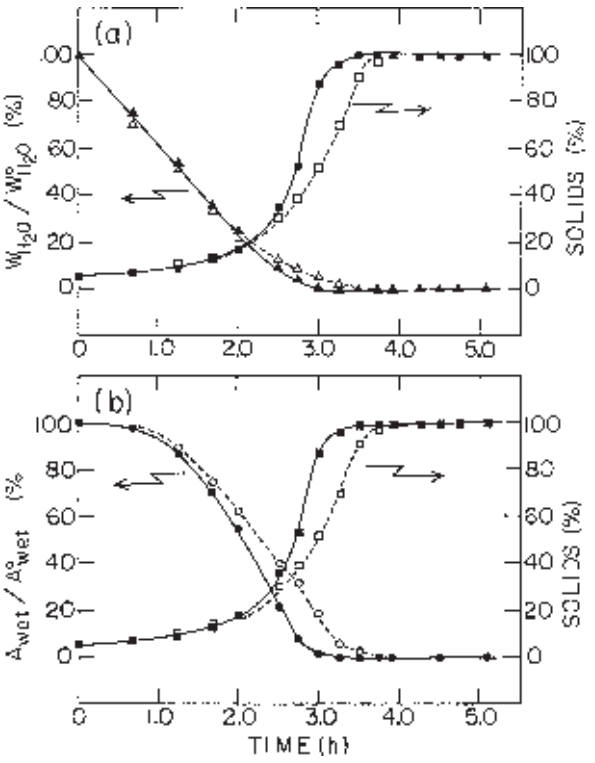

Figure 6—The drying process for a dispersion of soft latex (d = 43 nm, T_g = –33°C, open symbols*) and of hard latex (PMMA, d = 110 nm,* filled symbols*). In (a) the percent solids* (squares*) and the fraction of water remaining* (triangless*) are plotted, while in (b) we plot the relative area of the wet dispersion* (circles*), as a function of time. Both dispersions are surfactant-free.*

the propagation of the drying front during the entire process from a dilute dispersion to a solid film. An example of one of our experiments is given in *Figure* 6, where we show drying curves for two latex samples, one hard and one soft. We plot in *Figure* 6a the solids content (in weight percent) and the fraction of water remaining (W_{H2O}/W^o_{H2O}, in %) in the latex samples as a function of time. In *Figure* 6b, for the same samples, we compare the area of the wet region relative to its initial value (A_{wet}/A^o_{wet}, in %) as a function of time. The plots of solids content versus time are sigmoidal, with a slow upward curvature, and a sharp break as the lines approach 100% solids. Initially, the solids content changes slightly with time. This is a consequence of starting the experiment at a low solids concentration: when half the water has evaporated, the solids content has only increased from 5 to 10 wt%. In the very beginning, the wet area does not change very much, but after about 40 min, a dry edge appears, and the drying front starts to move inward.

Over the first 2.5 hr, the weight fraction of water remaining in the dispersion decreases linearly with time. The linearity of water loss persists even when the measured wet area has decreased by a significant extent (e.g., by 60% of its initial value). This implies that water evaporation occurs not only in the wet dispersion part, where water loss rate (g min^{-1}) is proportional to the surface area, but also in other regions of the film, which must be near the wet-dry boundary. We will discuss this important issue in the following. After 2.5 hr, when the solids content has reached 30 wt%, the wet area has already decreased to 30% of its initial value. At this point, the rate of water loss for both dispersions begins to decrease, characterized by non-linearity in the water loss curves. Further water loss corresponds to a large, rapid increase in solids content. Above 60 to 80% solids, there is a marked slowing of the water evaporation rate. The wet drop is very much reduced in size and disappears during this stage of the drying process. The solids content eventually reaches its equilibrium value (typically 97-99%).

Once these latex films become transparent or apparently dry to the eye, no further weight decrease is detected during further aging in air. The residual water content, measured by the weight lost during heating the films under vacuum, is small (< 3 wt%). This result differs from that reported by

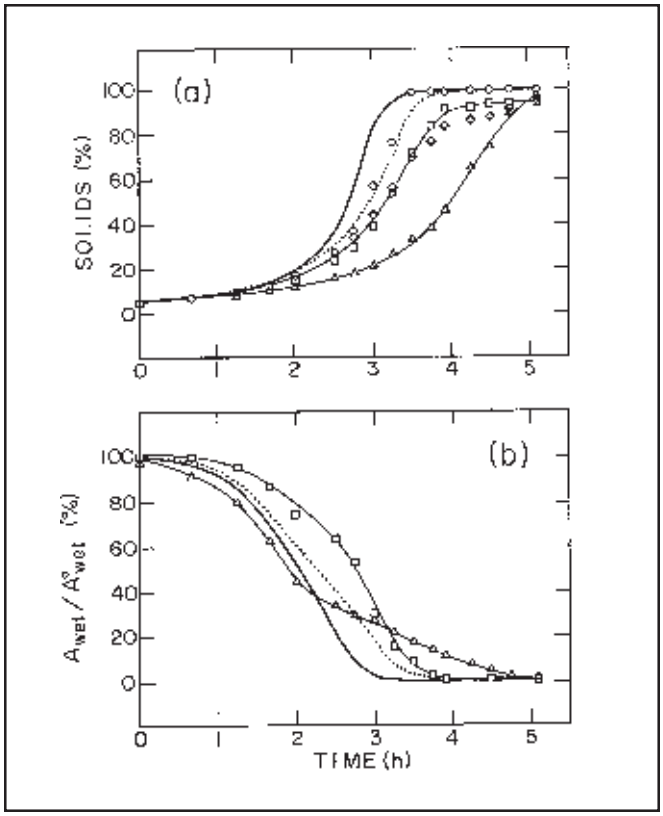

*Figure 7—Drying curves for surfactant-free blends of various weight fractions of hard component: (a) growth in percent solids as a function of time for dispersions of a hard latex (*solid line*), a soft latex (*dashed line*), and blends of Φ_{hard} = 0.33 (*squares*), 0.47 (*diamonds*), 0.56 (*Δ*), and 0.78 (*circles*). (b) Decrease in wet area during drying, showing the movement of drying front for dispersions of pure hard latex (*solid line*) and pure soft latex (*dashed line*) and latex blends of Φ_{hard} = 0.33 (*squares*) and 0.56 (*triangles*). The soft and hard latex dispersions used for preparing the blends are those of Figure 6. Note that $\Phi_{hard} = (1 - \Phi_{soft})$.*

Vanderhoff,[11] who observed significant water loss (~ 10 wt%) over a prolonged aging period.

An interesting observation is that the drying front moves at different rates during the experiment. At very early times, there is only a wet dispersion. After a certain period (here, 40 min), the dry edge appears. The propagation of the drying front is initially slow, but becomes rapid at the transition region where most of the water has evaporated, and the polymer changes from the minor to the major component. Near the end of the drying process, the propagation rate diminishes. Finally the liquid dispersion fades, and the wet area approaches zero. One can see that the rapid rate of decrease in the area of the wet drop (t = 1.5 to 3 hr in *Figure* 6b) precedes the rapid rate of increase of latex solids (t = 2.5 to 3.5 hr) in the system.

The most interesting result in *Figure* 6 is that the dispersion of PMMA particles dries significantly faster than that of the P(BMA-co-BA) latex with a T_g below room temperature. This difference may be a matter of particle size, or, as we show in the following, a fundamental difference in behavior between dispersions of hard and soft latex particles. In the cases we have examined, dispersions of latex with T_g well above room temperature often dry more rapidly than dispersions of low T_g latex.

DRYING OF LATEX BLENDS

Latex blends were prepared by mixing dispersions of a hard latex with those of a soft latex. *Figure* 7 shows drying curves for a set of surfactant-free dispersions, in which percent solids is plotted versus time in *Figure* 7a, and the relative wet area is plotted versus time in *Figure* 7b.

The first feature one notices in the drying curves is that latex blends dry differently from the dispersions of soft and the hard latex alone. As seen in *Figure* 6, the hard latex dispersion dries faster than the dispersion of soft latex. One might imagine that blending these samples would lead to intermediate drying rates. What one observes is that for most of the compositions studied, the blends dry much slower than the dispersions of either pure component. As the weight fraction of hard component increases from 0 to 0.56, the time taken for the dispersions to reach high solids increases systematically, implying a decrease in drying rates. One also observes that the drying front propagates more slowly for blend samples with Φ_{hard} below ~0.5 than that for either the soft or hard latex dispersion (cf. Φ_{hard} = 0.33 in *Figure* 7b). It is only when the blends become non-film forming (e.g., Φ_{hard} = 0.78), that they exhibit rapid drying.

We also observed a decrease in the drying rate in blends in which the hard latex was replaced by samples of d_{hard} = 167 or 44 nm, and when the soft latex was replaced with a sample of d_{soft} = 49 nm and T_g = 9.9°C.

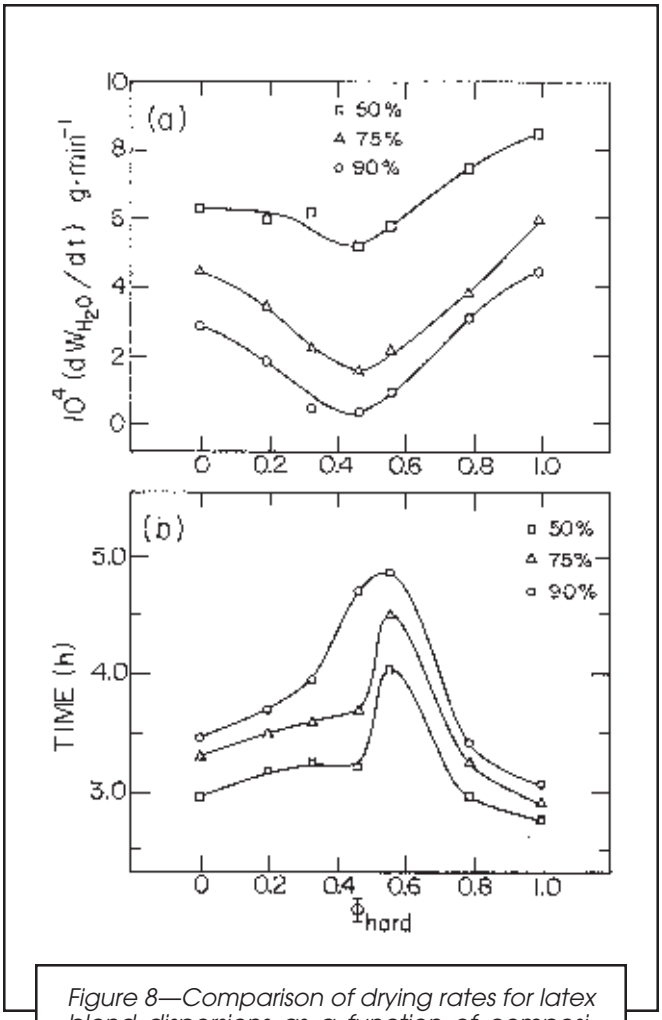

Figure 8—Comparison of drying rates for latex blend dispersions as a function of composition: (a) instantaneous water evaporation rates (g.min^{-1}) at 50, 75, and 90 wt% solids; (b) the time taken (in hr) during drying for each dispersion to reach 50, 75, and 90 wt% solids. The data are derived from Figure 7.

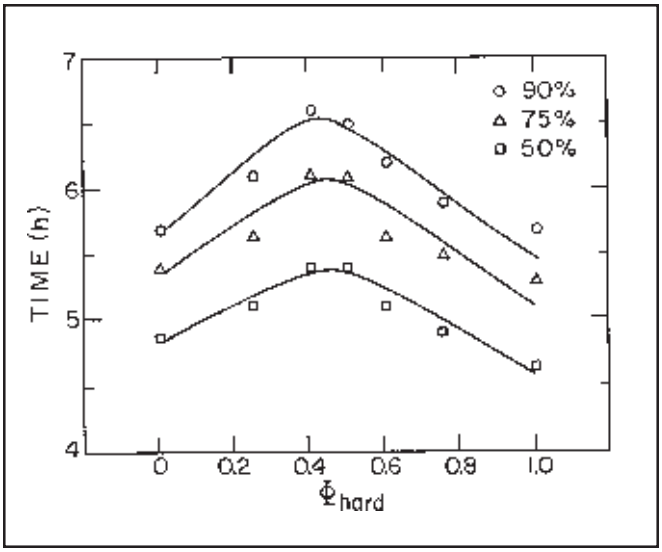

Figure 9—Comparison of drying rates for SDS-containing latex blends as a function of composition: the time taken (in hr) during drying for each dispersion to reach 50, 75, and 90 wt% solids. The samples are identical to those in Figures 7 and 8 except that 6 wt% SDS, based upon latex solids, has been added to the initial dispersion.

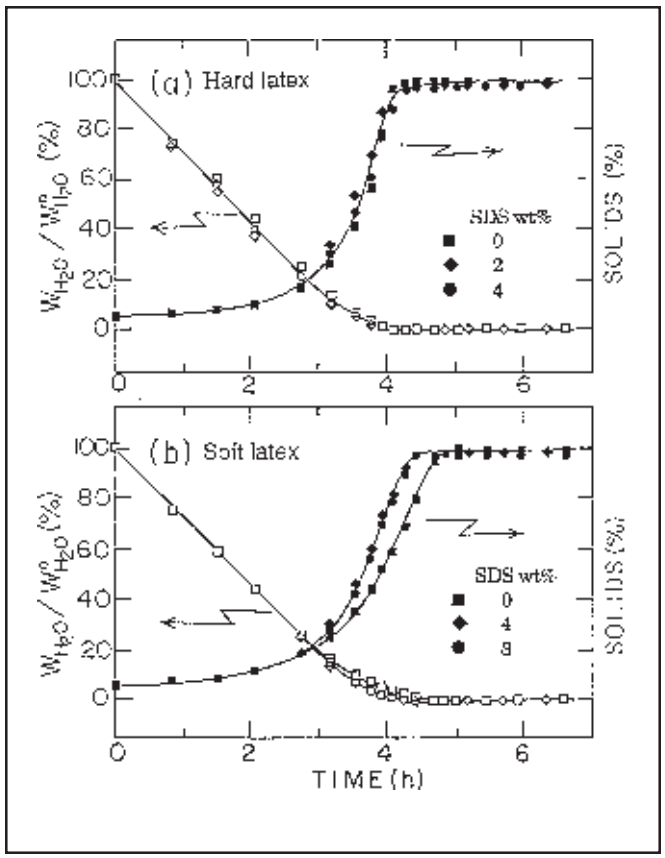

Figure 10—Comparison of the drying process, with and without SDS, for soft and hard latex dispersions: (a) drying curves for a surfactant-free PMMA latex (d = 110 nm, squares*) and samples with post-added SDS: 2 wt% (*diamonds*), 4 wt% (*circles*); (b) drying curves for soft latex (d = 43 nm, T_g = –33°C) dispersions containing 0 wt% (*squares*), 4 wt% (*diamonds*), and 8 wt% (*circles*) SDS. The amount of surfactant is calculated based upon latex solids.*

There are two ways to appreciate the effect of composition on the drying rate. First, the drying process can be characterized by the instantaneous water evaporation rate, i.e. the slope at each point in the water loss curve. For a series of different blends, these water-loss rates can be compared among samples of identical solids content. In *Figure* 8a, we plot the water-loss rate vs Φ_{hard}, comparing samples at 50, 75, and 90 wt% solids. A second measure of the drying rate is the time needed to reach a given solids content. This comparison is shown in *Figure* 8b.

We note that there is a distinct composition at which the drying occurs at the slowest rate. At 50 wt% solids, samples of Φ_{hard} = 0.47 and 0.56 have a decreased water evaporation rate. Only the two non-film forming samples (Φ_{hard} = 0.78 and 1) exhibit a significantly faster evaporation rate than that measured for samples of Φ_{hard} less than or equal to ~0.55. More pronounced effects are seen at the later stages of drying. At both 75 and 90% solids, the water evaporation rates exhibit a clear minimum at Φ_{hard} close to 0.5.

The same trend is seen in *Figure* 8b. There is a peak in each plot of the global drying time versus Φ_{hard} at various solids contents, representing the slowest rate of drying. There is also a small shift in the peak position, from $\Phi_{hard} \cong 0.5$ in *Figure* 8a to $\Phi_{hard} \cong 0.55$ in *Figure* 8b. What is particularly curious about this system is that the blend with Φ_{hard} = 0.56 dries very differently from those of lower values of Φ_{hard}. For example, in *Figure* 7a one finds that water evaporation of this sample occurs very slowly at early times (t < 2.5 hr) and after 2.5 hr, it dries more rapidly. The overall drying time for this sample is the longest, but the instantaneous drying rate at 50, 75, and 90 wt%, respectively, is not the slowest. In contrast, the dry edge is fast to develop at early times and the wet center shrinks more slowly in the later stages than for the samples of Φ_{hard} = 0.33 (or 0.47), as seen in *Figure* 7b. Because we were surprised, we repeated these experiments several times and this behavior is reproducible.

Surfactant Effects on the Drying Rate

Figure 9 shows corresponding data for surfactant-containing dispersions. These are the same samples shown in *Figures* 7 and 8 but with 6 wt% SDS present, based upon latex solids. The drying behavior observed is similar to that seen in *Figure* 8: with increasing Φ_{hard} the drying rate passes through a minimum. These dispersions show a narrower range of drying rates than those without surfactant. This points to a surfactant effect on the drying rate itself, which is described in more detail in the following.

Figure 10 presents comparisons between latex dispersions with and without surfactant (SDS). Both series were dried at the same time and under identical conditions. In the case of hard latex (d = 110 nm), there is no significant difference between the SDS-free sample and those with post-added 2 and 4 wt% SDS, respectively. For soft latex (d = 43 nm, T_g = –33°C), addition of 4 wt% SDS to the surfactant-free dispersion leads to an increase in the drying rate. Further increases in SDS content up to 8 wt% has no additional effect on the drying rate.

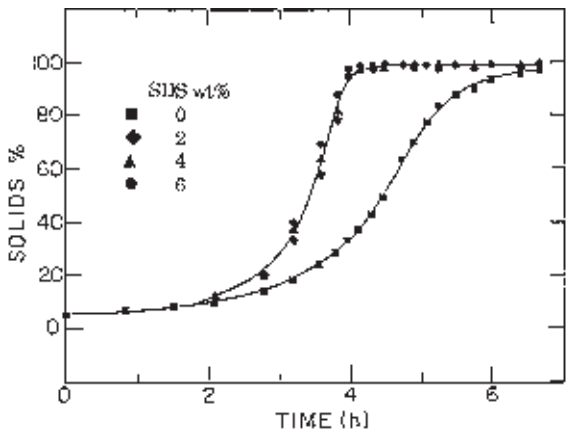

*Figure 11—Comparison of the drying process, with and without SDS, for latex blend dispersions containing 0 wt% (*squares*), 2 wt% (*diamonds*), 4 wt% (*triangles*), and 6 wt% (*circles*) SDS. The blends contain a 1:1 weight ratio of soft latex (d = 43 nm and T_g = –33°C) and PMMA (d = 110 nm).*

The previously mentioned results indicate that the drying rate of soft latex dispersions is sensitive to the presence of SDS, but, above a certain amount, is insensitive to the amount present. Another interesting point is that for surfactant-free samples, the hard latex dispersion dries significantly faster than that of the soft latex (4 hr for the hard latex, and 4.75 hr for the soft latex dispersion to reach 97 wt% solids), whereas in the presence of SDS their drying rates become very similar.

We emphasize this point in *Figure* 11, where we show the drying curves for blends of $\Phi_{hard} = 0.5$ with different amounts of SDS. The surfactant-free sample dries much slower than the surfactant-containing samples. When 2, 4, and 6 wt% SDS were added into the latex, the drying becomes much faster, but is again independent of the SDS amount. Isaacs[16] also reported that surfactant accelerates water evaporation during the late stages of film formation. What is curious here is that the amount of surfactant needed to promote the drying rate is less than that needed for monolayer coverage of the latex. Coverage can be estimated by assuming that the area per SDS molecule at saturation is 0.8 nm^2 on a PMMA surface and 0.6 nm^2 on PBMA or PBA.[17] For monolayer coverage, one needs 2.7 wt% SDS for 110 nm PMMA latex particles, and 11 wt% for 43 nm P(BMA-co-BA) latex particles. In *Figures* 10 and 11, we see that 2-4 wt% SDS is enough to increase the drying rate for the dispersion of tiny P(BMA-co-BA) latex particles.

MODELS FOR THE DRYING PROCESS

The previous results indicate that there is a distinct composition in latex blends at which the dispersion dries at a slowest rate. For the dispersions examined, this composition corresponds to a Φ_{hard} value close to 0.5. We have some evidence that for very small PMMA particles (44 nm), the minimum is shifted to a lower value of Φ_{hard}. This retardation in drying rate represents a fundamental feature of film formation which must be accommodated into realistic models of the drying process.

Classic Models of Drying

The classic model for the drying process for latex dispersions was proposed by Vanderhoff.[11] He discerned three regions in the plot of cumulative water loss versus drying time. In stage 1, in which the particles remain separated, water evaporates at its normal rate from the surface of the dispersion. Stage 2 commences as the particles come into close contact. The water evaporation rate slows as the particles deform, and the surface area of the water pool decreases. Eventually, coalescence leads to closing of the surface. In stage 3, the loss of the last traces of water is very slow because the water now must diffuse through the continuous polymer phase.

Other models have been put forward for the drying process, for example by Croll,[12] and more recently by Rudin.[18] The Croll model also treats the drying process as occurring uniformly across the surface, with a flocculated phase separating the wet dispersion from the air. Rudin modified the Croll model to include skin formation across the surface of the dispersion during drying.

The Vanderhoff model is often cited and has an appealing simplicity and generality. It and the Croll model, however, overlook important aspects of the drying process. These models presume, for example, that drying is uniform and neglects the propagating drying front. The Vanderhoff model suggests that water evaporates at the same rate from the dispersion as from a liquid water surface, and continues to evaporate at this rate until the meniscus of the water approaches the tops of the particles in the film. This view is problematic because the area of the wet portion of the film contracts during drying.

Recent Views of the Drying Process

It is important to mention here two sets of experiments described in the recent literature. First, a group at Rhône-Poulenc examined the role of polar material at the surface of latex particles in the film formation process.[14] This material forms an interconnected membrane in newly formed films. If the membrane phase is sufficiently robust, or if the film is examined shortly after drying, the membrane can be rehydrated. Neutron scattering experiments on films rehydrated with D_2O give diffraction peaks corresponding to the size of the original latex particles, implying that a continuous network of membranes persists throughout the film. Note the implication that the latex particles deform before they come into contact, a result which receives strong support from recent experiments reported by Crowley et al.[19] We believe that the structure of this kind of interconnected membrane

MITCHELL A. WINNIK is Professor of Chemistry at the University of Toronto. He received the B.A. Degree from Yale University and the Ph.D. Degree from Columbia University. After a postdoctoral year at the California Institute of Technology, Prof. Winnik joined the faculty at Toronto in 1970 and undertook studies in the area of organic photochemistry. He began research in the polymer field in 1978. Current efforts in his research group focus on the development of new techniques to study polymer surfaces and polymer interfaces as well as coalescence phenomena in latex films. In 1993, Prof. Winnik presented the Canadian Institute of Chemistry Macromolecular Science Award Lecture, sponsored by Nova Corporation. In 1995, he received the Canada Bell Forum Award, sponsored by The Corporate Higher Education Forum for excellence in university-industry collaborative research.

JIANRONG FENG graduated from Beijing University, in China, in 1985. He received the M.Sc. Degree in Polymer Science from the Chinese Academy of Sciences in 1988. After a short stay as a visiting scholar (from 1991) working with Prof. Winnik at the University of Toronto, he began graduate studies and he is currently a Ph.D. student in Prof. Winnik's lab. Mr. Feng's submission for the Sherwin-Williams Student Award Competition, administered through the Division of Polymeric Materials of the American Chemical Society, has been selected as a finalist. His current research focuses on latex coatings.

must be important for determining the drying rates during film formation.

The second set of experiments come from a Japan-Bulgaria collaboration investigating the forces which cause spherical particles in dispersion to form ordered monolayers upon drying. Denkov et al.[15] monitored the drying of micron-sized polystyrene latex dispersions by optical microscopy. They observed a convective flux of the particles tending to form a close-packed particle phase, and the direction of particle motion depended on whether the liquid droplet was concave or convex in shape. On a flat glass surface where the liquid film was convex, particle accumulation occurred first at the edge. The particle arrays built up at the periphery as a result of a particle flux from the droplet toward the boundary. When a concave liquid was formed inside a Teflon ring, the formation of close-particle-packing started from the central part of the dispersion. This group argued that once the particles came in contact with the substrate so that they protruded from the water surface, the high surface area would lead to enhanced evaporation from this region, with capillary forces supplying water from the droplet. This in turn sets up a flux of water from the droplet to the drying edge, transporting latex from the bulk to the edge. When the drying rate is sufficiently slow, the forces involved are enough to lift particles above the dried particle layer at the edge, making the final particle layers thicker at the edge than in the center.

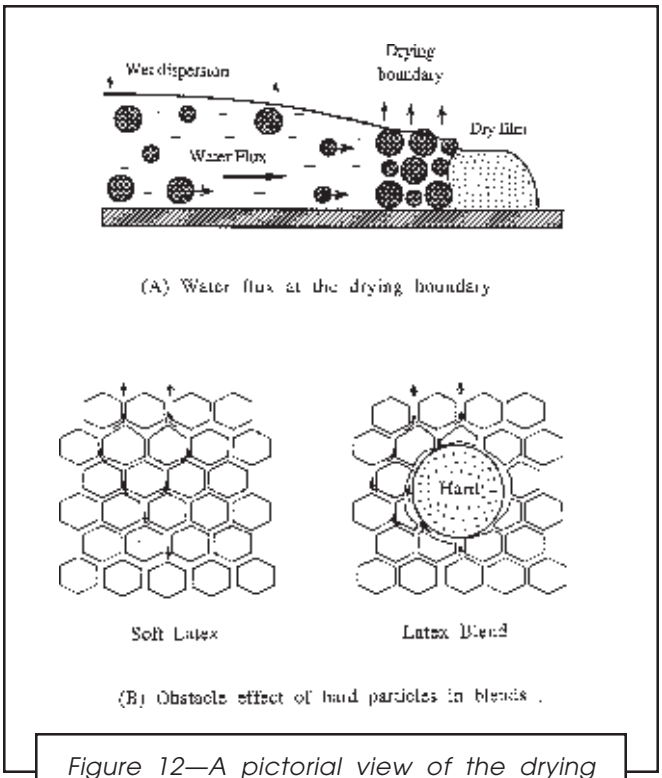

Figure 12—A pictorial view of the drying mechanism. In (a) we show that there is convective flow of water towards the drying boundary and fast evaporation of water in this region due to its high surface area. In (b) we show that as a film forms from soft latex, water is transported through the hydrophilic membrane between the particles. In the blends, hard particles form obstacles and act as a barrier to capillary transport.

This description of the drying mechanism accommodates two key features of the process which other models cannot explain. First, it explains the origin of the drying front and the direction of its propagation. Second, it explains the observation that films formed on flat glass substrates are often thicker at the edges than in the center, especially at slow evaporation rates.

Our View of the Drying Process

From the previously mentioned point of view, the reason that dispersions of hard latex dry faster than those of similar-sized soft latex is related to the magnitude of the capillary transport of water at the wet-dry interface. High T_g latex do not deform during drying. The pore structure that remains can conduct water from the wet domain into this high surface area region of the film. Deformation of the soft latex will lead to smaller capillaries and reduced flow of water. When surfactant is present, it would form a hydrophilic membrane, and this would have a larger effect on the capillary of the soft latex than on the larger pores formed when the hard latex dispersions dry.

In latex blends, the soft latex can deform to fill the spaces between the hard particles. At low values of Φ_{hard}, the hard particles act as obstacles to the diffusion of water through the capillaries of the soft latex matrix. Obstacles decrease the diffusion or capillary flow rate by increasing the tortuosity of the path.[20] At high values of Φ_{hard}, the soft latex polymer plugs the pores between the hard latex. This also produces obstacles to water flow, and the drying rate is slower than for the hard particle dispersion itself.

A somewhat similar observation was reported many years ago by Sullivan[21] on evaporation of organic solvents from the newly dried pigmented latex films. He found that organic solvents (e.g., ethylene glycol) evaporated slowest from the nearly dried films when the pigment volume concentration (PVC) was ~50%. In these pigmented latex systems, the major components are the hard, large pigment particles and the soft binder latex. There is also a critical volume concentration (CPVC) of the pigment particles at which the polymer phase changes from continuous to discontinuous, which is also close to 50%.[22,23] Sullivan explained that large pigment particles gave rise to circuitous pathways and more resistance for organic solvent transport when PVC < CPVC, while the fast evaporation observed when PVC > CPVC was also attributed to the presence of large voids.

To summarize, as water evaporates from a latex dispersion, a dry edge forms at the thinnest portion of the wet film. Drying occurs as a propagating front because water evaporates more rapidly from the high surface area region at the wet-dry boundary than from the wet surface of the droplet itself. Water is constantly wicked through the pore structure to this dry region, and this in turn creates a flux of water and particles from the droplet to the dry edge. In *Figure* 12a we present a pictorial view of the flux of water and particles toward the drying boundary where fast evaporation occurs. This view may be modified for the case in which salts and surfactant have been removed from the system. Here there can be strong long-range forces between the latex particles in the liquid droplet. These can slow down the flux of particles toward the edge, and if a colloidal crystalline phase is formed, particle transport may be suppressed. In *Figure* 12b we show that as a film forms from soft latex, water is transported through the

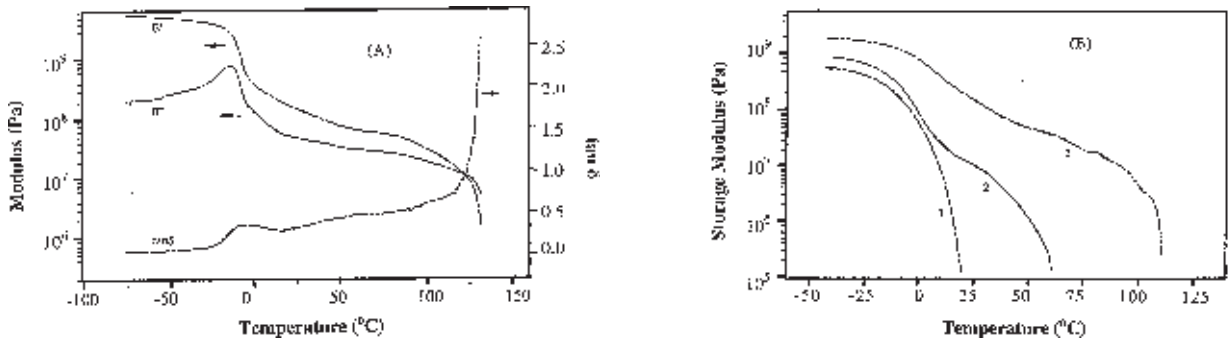

Figure 13—Dynamic mechanical analysis of latex films composed of 110 nm PMMA particles and P(BMA-co-BA) soft polymer: (a) Log plots of E′, E″, and tan δ versus T under controlled-strain conditions (strain 0.04%, frequency 1 Hz) for a latex blend film of Φ_{hard} = 0.5; (b) Log plots of the dynamic storage modulus (E′) versus temperature (strain 0.025%; frequency 1 Hz) for films consisting of different amounts of hard component. Curves 1, 2, and 3 refer to Φ_{hard} = 0, 0.25, and 0.5, respectively.

hydrophilic membrane between the particles, and in blends, hard particles act as a barrier to the water transport and hence reduce the evaporation rate at low Φ_{hard}.

From the systems examined in *Figures* 7-9, we see that dispersions with a composition near Φ_{hard} = 0.5 dry at the minimum rate. Note that this composition lies in the same range as the critical composition (close to 0.5) at which the films formed from dispersions change from continuous, transparent to turbid (see *Figure* 1). We suspect that there is a connection between more rapid water loss for larger values of Φ_{hard} and the onset of turbidity in the films. Turbidity indicates the presence of voids which the soft latex is unable to fill completely. These voids can act as conduits for water transport during the later stages of drying and water evaporation occurs fast as Φ_{hard} increases from ~0.5 to higher values.

MECHANICAL PROPERTIES

One of the reasons that latex blend films represent a useful strategy for zero VOC coatings is that the films have enhanced mechanical properties. There appears to be a strong interaction between the hard latex and the soft matrix, which gives useful mechanical coupling between them. In this section, we examine briefly the nature of this interaction.

Blend films of PMMA and P(BMA-co-BA) were investigated by dynamic mechanical analysis (DMA). *Figure* 13a shows a typical result for a blend film sample with Φ_{hard} = 0.5. We show changes in the storage modulus E', the loss modulus E", and loss tangent (tan δ) versus T (°C). The first transition, characterized by the sharp decrease of E', and peaks for E" and tan δ at about –10°C, reflects the glass transition of the soft component. The second transition occurs at T > 110°C, where the PMMA hard particles begin to soften, and the composite starts to flow. The most interesting information comes from comparing samples from different blend compositions. For this purpose, in *Figure* 13b we plot the storage modulus versus temperature for film samples with Φ_{hard} = 0, 0.25, and 0.50, respectively.

There are several noteworthy features in *Figure* 13. First, we see that the overall film modulus is significantly increased when the soft polymer is blended with the hard latex. Second, the high modulus region of the DMA spectrum extends to a much higher temperature when the hard component is present. In addition, the glass transition of the soft component becomes broader and shifts to higher temperature when the amount of hard particles increases, indicating that the physical properties of the soft polymer itself have been modified due to the interaction with the hard particles. These results are of particular importance for the use of latex blends in coatings. These dispersions form films at room temperature without the need for any coalescing aid, yet the films that form have a much higher modulus at room 22°C (E' on the order of 10^8 Pa) than the low T_g latex polymer.

The dynamic mechanical properties of these latex blend films resemble those of polymers compounded with inorganic filler. Physical models[24,25] of polymer/filler systems invoke the idea that a layer of soft polymer adjacent to a hard surface becomes stiffer. NMR studies[26,27] reveal that there is a reduction of molecular mobility of the soft polymer adjacent to the filler particles that causes the shift of glass transition position and the increase of the modulus of the matrix. When the volume fraction of hard particles increases, the fraction of soft component that is influenced by the hard particles increases, and the effect of reinforcement becomes more pronounced.

The PMMA particles in the soft polymer matrix act as reinforcing filler in our blend films. They increase the modulus, the hardness and the block resistance of these films. This effect is rather remarkable, considering that there is no obvious source of chemical interaction between the components, as one would have between an acrylate polymer and a silica or TiO_2 surface. These are dissimilar polymers, and if one had only van der Waals interactions at the surface, one might imagine that the adhesion forces would be rather weak.

CONCLUSIONS

Latex blend films were prepared from dispersions containing a mixture of hard and soft latex particles. For films spread on a flat glass surface, the drying process exhibits a drying front which propagates from the edge towards the center. Dispersions of soft latex dry more slowly than those of a corresponding latex with a T_g above room temperature. Blends of these

dispersions take longer to dry, and there exists a distinct composition which dries at the slowest rate. The presence of surfactant facilitates the water evaporation rate. We propose a model to explain the drying mechanism.

Transparent films are obtained when sufficient soft component is present. This corresponds to the concentration at which it becomes the continuous phase. The surface and bulk morphologies, studied by atomic force microscopy, scanning electron microscopy, and freeze-fracture transmission electron microscopy, reveal that transparency of the films corresponds to a random distribution of hard spheres in the soft matrix. An intimate contact is achieved between the two polymer phases. In these blend films, the hard particles act as a reinforcement filler and provide a remarkable improvement in the mechanical properties of the films formed.

ACKNOWLEDGMENTS

The authors thank the Institute of Chemical Sciences and Technology, NSERC Canada, and the Province of Ontario for their support of this research. We thank Professor J. Vancsco for assistance with the DMA measurements.

References

(1) Karsa, D.R., *Additives for Water-Based Coatings*, Royal Society of Chemistry, London, 1991.
(2) Broek, A.D., *Prog. Org. Coat.*, 22, 55 (1993).
(3) Winnik, M.A., Wang, Y., and Haley, F., "Latex Film Formation at the Molecular Level: The Effect of Coalescing Aids on Polymer Diffusion," JOURNAL OF COATINGS TECHNOLOGY, *64*, No. 811, 51 (1992).
(4) Feng, J., Winnik, M.A., Shivers, R., and Clubb, B., *Macromolecules*, 28, 7671 (1995).
(5) (a) Friel, J., European Patent Application, 0466 409 A1 (1992); (b) Snyder, B.S., U.S. Patent 5308890 (1994).
(6) Patel, A., Feng, J., Winnik, M.A., Vancso, J., and McBain, C., *Polymer*, 1995, in press.
(7) Wang, Y., Kats, A., Juhué, D., Winnik, M.A., Shivers, R., and Dinsdale, C., *Langmuir*, 8, 1435 (1992).
(8) Bohn, L., in *Polymer Handbook, 2nd Edition*, Brandrup, J. and Immergut, E.H. (Eds.), , Wiley-Interscience, NY, p. 111-211, 1975.
(9) Rosen, S.L., *Polymer Eng. Sci.*, 7 (2), 115 (1967).
(10) Mark, H.F., Bikales, N.M., Overberger, C.G., and Menges, G., *Encyclopedia of Polymer Science and Engineering, Vol. 1*, John Wiley and Sons, New York, p. 257, 1985.
(11) Vanderhoff, J.W., Bradford, E.B., and Carrington, W.K., *J. Polymer Sci.: Symposium No. 41*, 155 (1973).
(12) Croll, S.G., "Drying of Latex Paint," JOURNAL OF COATINGS TECHNOLOGY, *58*, No. 734, 41 (1986).
(13) Pramojaney, N., Poehlein, G.W., and Vanderhoff, J.W., *Drying'80, Vol. 2*, p. 93-100, 1980.
(14) Chevalier, Y., Pichot, C., Graillat, C., Joanicot, M., Wong, K., Lindner, P., and Cabane, B., *Colloid Polymer Science*, 270, 806 (1992).
(15) Denkov, N.D., Velev, O.D., Kralchevsky, P.A., Ivanov, I.B., Yoshimura, H., and Nagayama, K., *Langmuir*, 8, 3183 (1992).
(16) Isaacs, P.K., *J. Macromol. Chem.*, 1, 163 (1966).
(17) Vijayendran, B.R., *J. Appl. Polymer Sci.*, 23, 733 (1979).
(18) Eckersley, S.T. and Rudin, A., *Prog. Org. Coat.*, 23, 387 (1994).
(19) Crowley, T., Sanderson, A., Morrison, J., Barry, M., Morton-Jones, A.J., and Rennie, A.R., *Langmuir*, 8, 2110 (1992).
(20) Mackie, J.S. and Meares, P., *Proc. R. Soc. London*, A 1955, 232, 498.
(21) Sullivan, D.A., "Water and Solvent Evaporation from Latex and Latex Paint Films," JOURNAL OF PAINT TECHNOLOGY, *47*, No. 610, 60 (1975).
(22) Stieg, F.B., *Prog. Org. Coat.*, 1, 351 (1973); Stieg, F.B., "Particle Size as a Formulating Parameter," JOURNAL OF PAINT TECHNOLOGY, *39*, No. 515, 701 (1967).
(23) Schaller, E., "Critical Pigment Volume Concentration of Emulsion Based Paints," JOURNAL OF PAINT TECHNOLOGY, *40*, No. 525, 433 (1968).
(24) Mations, V.A., *Polymer Eng. and Sci.*, 9, 90 (1969).
(25) Vollenberg, P.H.T. and Heikens, D., *Polymer*, 30 (9), 1656 (1989).
(26) Douglass, D.C. and McBrierty, V.J., *Polymer Eng. and Sci.*, 19, 1054 (1979).
(27) Mahoney, D. and Meerwall, E.V., *J. Polymer Sci. Polymer Phys.*, 31, 1029 (1993).